Projected Change in Mean and Extreme Climate over Korea from a Double-Nested Regional Climate Model Simulation

Eun-Soon IM, Moon-Hyun KIM, Won-Tae KWON

Climate Research Team, National Institute of Meteorological Research, Korea Meteorological Administration, Seoul, Korea

and

Steven COCKE

Center for Ocean-Atmospheric Prediction Studies, The Florida State University, Tallahassee, Florida, USA

Abstract

We present an analysis of a simulated climate projection covering the period 1971–2080 over the Korean Peninsula with a regional climate model (RegCM3) using a one-way double-nested system. The mother and nested domain cover the East Asian region at 60 km grid spacing and the Korean Peninsula at 20 km grid spacing, respectively. The mean climate state as well as the frequency and intensity of daily extreme events are investigated at various temporal and spatial scales, with a focus on surface air temperature and precipitation. Our analysis is primarily centered on the comparison of two 30-year climate periods between 2021–2050 and 2051–2080, in order to assess climatic changes at different time periods in response to anthropogenic forcings under the IPCC B2 emission scenario.

Regarding the interdecadal variation of projected temperature and precipitation over the whole integration period, we find that the temperature change gradually increases by 3.2 K for the 2070s, with a persistently increasing trend. The projected precipitation in the future shows generally greater amounts than in the reference run despite significant interdecadal variation. A substantial increase (decrease) of hot (frost) spells is projected along with increasing of maximum and minimum temperature. Wet spells of long periods tend to be more frequent, accompanying the increase of precipitation amounts. The temperature changes are statistically significant at the 90% confidence level in all seasons and regions, indicating robustness of the projected change while the precipitation changes show low statistical confidence, especially summer season, due to the large natural variability. Based on the spatial distribution, although the general pattern between the mother and nested domain simulations shows similarity, more detailed structure over Korea is found in the nested domain simulation. By comparison of the change between 2021–2050 and 2051–2080 periods, the climate change signal of both temperature and precipitation becomes more pronounced in the late 21st century as the greenhouse gas concentration is increased.

1. Introduction

It has been well known that the global average surface temperature has increased by 0.6 K since the late 19th century due to anthropogenic influence through the emission of greenhouse gases and other radiatively active gases (IPCC 2001). The climate of Korea

Corresponding author and present affiliation: Eun-Soon Im, Earth System Physics, Abdus Salam International Centre for Theoretical Physics, Trieste, Italy.
E-mail: esim@metri.re.kr

also has experienced a gradual warming (Oh et al. 2004), as indicated by a significant warming trend from the observed record. In South Korea, the increasing rate of the average temperature is reported to be about 1.5 K during the 20th century mainly due to the greenhouse effect and rapid urbanization (Kwon 2005), which is almost three times of global warming trend. This indicates that Korea will be strongly expected to be vulnerable to climate change (Oh et al. 2004; Boo et al. 2006). In fact, there is discernable evidence that recent climate changes over Korea have already affected many environmental and biological systems (Boo et al. 2004; Im et al. 2007a).

In order to derive a meaningful interpretation about climate change and to project the potential future change, scenario simulations have been performed in numerous climate change studies (Gao et al. 2001; Gallardo et al. 2001; Giorgi et al. 2004a,b; Mearns et al. 1999; Oh et al. 2004; Räisänen et al. 2004; Kitoh et al. 2005; Kusunoki et al. 2006). Projections carried out based on future emission scenarios of greenhouse gases could provide useful insights for possible consequences due to climate change (Boo et al. 2004). To date, climate projections have been most widely simulated using coupled global climate models (GCMs) based on the IPCC SRES emission scenarios (IPCC 2000), with reasonable success (May and Roeckner 2001; Min et al. 2006). GCMs represent the broad features of current climate well and can reproduce the observed large-scale changes in climate over the recent past. Substantial problems arise, however, at the regional scale. In areas where coasts and mountains have a significant effect on the weather such as in Korea, scenarios based on GCMs will fail to capture the local detail needed for impact assessments at a regional level. Indeed, Korea is a representative region where the limitations of GCMs are particularly important, since the Korean Peninsula is small (the area of South Korea is 99,585 km^2) with a narrow mountain system surrounded by ocean, and since the climate of Korea is characterized by the occurrence of extreme precipitation episodes induced by orographical features (Part et al. 2003). Also, at such coarse resolutions, extreme events such as drought or heavy rainfall are either not captured or their intensity is unrealistically low.

One method for overcoming this limitation and adding detail to global projections is to use a regional climate model (RCM) (Christensen et al. 1998; Mearns et al. 1999).

With this background, we have developed the RegCM3 one-way double-nested system, with the mother domain encompassing the eastern regions of Asia at 60 km grid spacing and the nested domain covering the Korean Peninsula at 20 km grid spacing (Im et al. 2006, 2007a). We carried out the scenario experiments covering the period 1971–2080 using the ECHO-G B2 scenario simulation as the initial and lateral boundary conditions. A 110-year simulation is a long enough period to consider interdecadal variability of the model, which exhibit large fluctuations due to the external forcings of greenhouse gases. We first evaluated the reference scenario (1971–2000) against a dense observational network over the Korean territory (Im et al. 2007a). Im et al. (2007a) confirmed from this evaluation that the downscaled simulation (60 km and 20 km horizontal resolution) shows considerable improvement in the recent climate compared to the simulation from the GCM (approximately 350 km horizontal resolution). Subsequently, we have examined the potential future change for the 30-year period of 2021–2050 with respect the reference simulation (Im et al. 2007b). In this study, we extend the analysis period to consider the long-term variability. The multidecadal length of our simulations allows us to examine interdecadal variability and trends of the climate change signal, thereby providing a more reliable projection. Projections derived from a short period at a certain time in the future could lead to different interpretations of the results due to model variability, especially for precipitation where there may be large natural variability. Hence, we assess the possible future climate change with a focus on the two 30-year periods 2021–2050 and 2051–2080 based on the IPCC SRES B2 scenario with respect to a reference climate for a given baseline period (1971–2000). From a time-slice analysis, we can assess the climate change at different time periods in response to anthropogenic forcings. Our analysis is primarily centered on surface air temperature and precipitation, the two variables most used in impact assessment studies (Giorgi et al. 2004a). Emphasis in this

study is placed on the high-resolution spatial/ temporal aspects of mean and extreme climate change under different climate settings over Korea generated by complex topography and coastlines that are relevant on a regional scale. To this end, we will analyze the future climate change on various temporal scales, ranging from interdecadal to daily. It is expected that this study could provide useful insight into the future change signal as well as advance understanding of regional climate change over Korea.

In Section 2 we present a brief description of the modeling system and experiment design. The projected results for mother and nested domain simulation are then discussed in Section 3 and the summary and conclusions presented in Section 4.

2. Model and experiment design

Both global and regional climate models and the experimental setup used in this study are described in Im et al. (2007a,b) in detail, and the references therein. Therefore, we include only a brief description here.

The ECHO-G global climate model is used to provide the initial and boundary conditions, and consists of two component models, an atmospheric component ECHAM4 containing a land surface scheme and the oceanic component HOPE-G with an embedded sea-ice model. The horizontal and vertical resolution of ECHAM4 is spectrally truncated T30 (grid size approximately $\sim 3.75°$) and 19 hybrid sigma-pressure levels (highest level at 10 hPa), respectively. The horizontal resolution of HOPE-G corresponds to a Gaussian T42 grid ($\sim 2.8°$) and the model employs 20 vertical levels (Min et al. 2005). Analysis of results using the ECHO-G scenario (Oh et al. 2004) showed that the A2 [B2] scenarios over East Asia (defined as grid box of 80°E–180°E, and 20°N–60°N) by 2100 result in an increase in temperature of 6.5 [4.5] K and an increase in precipitation of 10.5 [6.0]%, respectively.

The regional model used here is the International Centre for Theoretical Physics (ICTP) RegCM3. This is an upgraded version of the model originally developed by Giorgi et al. (1993a,b) and then improved as discussed by Giorgi and Mearns (1999), and Pal et al. (2000). The regional model configuration, as well as a detailed evaluation of the present and recent climatology simulated by the RegCM3 one-way double-nested system, has been described by Im et al. (2006, 2007a). Figure 1 shows the model domain system used in this study. The
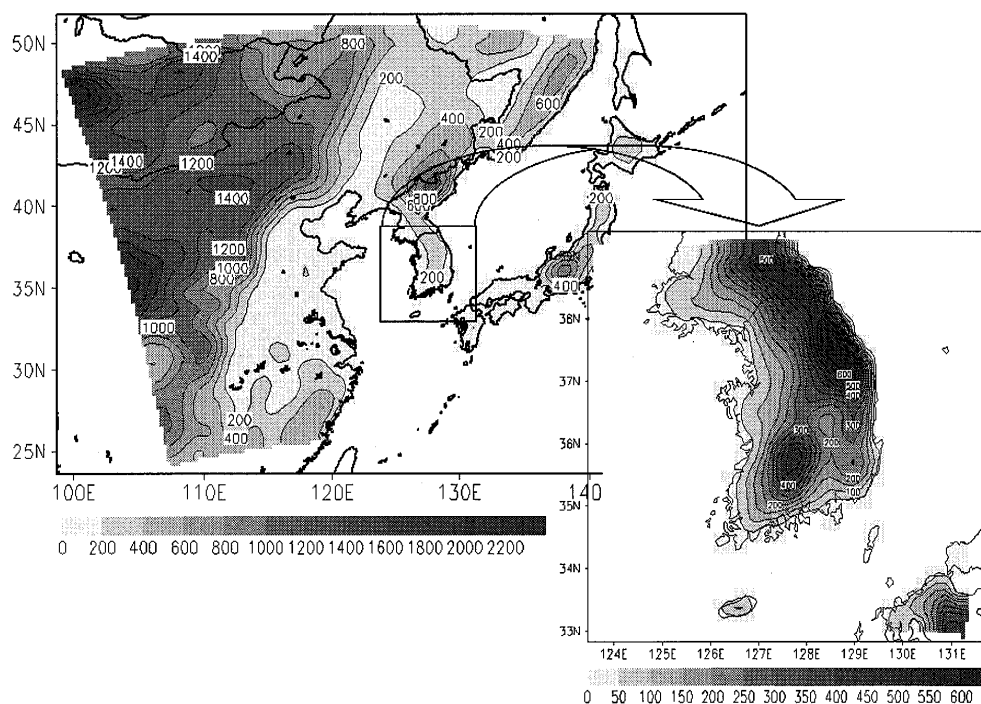

Fig. 1. Model domain and topography (m) for the mother (60 km grid spacing) and nested (20 km grid spacing) simulations.

mother domain covers the eastern regions of Asia (including the Korean Peninsula) at 60 km grid spacing, while the nested domain focuses on the South Korean Peninsula at 20 km grid spacing.

The integration spans the 110-year period of January 1971 through December 2080. Analysis is focused on the period 2021–2050 and 2051–2080. According to the B2 emission scenario, the CO_2, N_2O, and CH_4 mean concentration during 2021–2050 (2051–2080) (CO_2 = 447.2/515.1 ppm, N_2O = 342.4/354.9 ppb, and CH_4 = 2083.9/2383.5 ppb) are increased by about 29(49)%, 12(16)%, and 31(49)%, respectively, compared to the values during the reference period (CO_2 = 346.3 ppm, N_2O = 305.3 ppb, and CH_4 = 1596.0 ppb). The initial and time-dependent meteorological lateral boundary conditions are interpolated at 6-hourly intervals from the ECHO-G B2 scenario simulation which covered the period 1860–2100. Sea surface temperature (SST) over the ocean areas and major GHG concentration obtained from the corresponding ECHO-G fields are directly interpolated onto the RegCM3 grid system. The SST is updated monthly, and concentrations of major GHG vary every year.

3.　Results

Possible future changes in the mean climate state as well as in the frequency and intensity of extreme climate events due to emission forcing could be derived by comparing simulated current climate conditions as a baseline to simulated future climate states with increased GHGs (Meehl et al. 2000). Hence we compare changes by comparing relevant statistics (decadal and seasonal mean, daily frequency and intensity) for the future climate of two periods of 2021–2050 and 2051–2080 with respect to the present day period of 1971–2000.

3.1　Changes in mean climatology

We begin our analysis of the interdecadal variation of projected temperature and precipitation over the whole integration period for the purpose of determining the trend and persistence in the long-term variability of the change signal in response to increasing greenhouse gas concentration. Figure 2 presents the area-averaged decadal mean temperature and precipitation anomalies over Korea from the
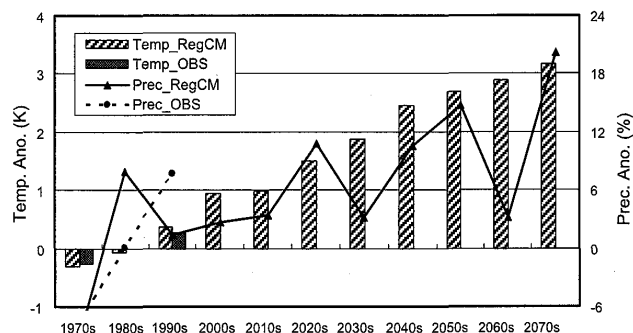

Fig. 2. Interdecadal variation of projected temperature and precipitation anomaly over Korea based on IPCC SRES B2 scenario.

nested domain simulation. Anomalies are computed with respect to the mean of the reference period (1971–2000).

For validation of the simulated results during reference period, we used the temperature and precipitation data at 57 climate stations archived at the Korea Meteorological Administration (KMA). The trend and variability of the simulated temperature during reference period illustrate remarkable similarity with those of the observation. According to the regional projection, it is clearly shown that temperature change gradually increases by 3.2 K for the 2070s, with a persistently increasing trend. In contrast to the temperature pattern, the precipitation change exhibits substantial variability. For the reference period, the observations show a fairly constant increasing trend through the last 30 years, whereas the reference simulation shows the maximum in the 1980s. Precipitation change does not show a well defined long term trend even though it generally has a positive anomaly in the future projection. Enhancement of variability is evident after 2020s. The projected precipitation in the future shows generally greater values than in the reference run and significant interdecadal variations with a large range of fluctuation instead of a regular trend throughout the simulation. This is a typical behavior of regional scale precipitation change (Giorgi 2005), and points to the need for carefully evaluating individual climate change simulations to establish the robustness of regional precipitation change signals.

Note that present scenario experiments have not included the land cover change and atmo-

spheric aerosols effects which may partially related to the biased temperature and precipitation results as shown by Fig. 2. The land use/land cover and atmospheric aerosols over East Asia including the Korean Peninsula have significantly changed in past several decades. The changes in land cover might have affected the albedo and the soil and vegetation functions and then could bring changes to the East Asian monsoon by altering the complex exchange of water and energy from surface to atmosphere (Fu 2003). Atmospheric aerosols also could influence the climate by inducing surface cooling throughout direct (scattering and absorbing solar radiation) and indirect (modifying the microphysical and optical properties of clouds) effects, especially over the East Asian region where the emission of aerosol have been rapidly increasing during the last decades (Qian et al. 2003; Giorgi et al. 2002, 2003).

In order to understand the difference concerning the synoptic-scale climate characteristics over East Asia during each period of increasing and decreasing precipitation as shown by Fig. 2, we perform a composite analysis of 850 hPa winds, water vapor flux, and 500 hPa

geopotential height. Circulation changes can modulate the patterns and magnitude of the surface climate in an important manner (Räisänen et al. 2004). The future precipitation change is mainly attributable to the change of wind fields in the horizontal transport of water vapor associated with the intensification of a subtropical high (Kusunoki et al. 2006). Figure 3 presents the difference in the 850 hPa winds, water vapor flux, and 500 hPa geopotential height between two composites (the average of two periods of increasing precipitation: 2051–2060 and 2071–2080/the average of two periods of decreasing precipitation: 2031–2040 and 2061–2070) and the reference (1971–2000) scenario for the winter and summer season.

Basically, the changes of the atmospheric circulation over East Asia modify the winter and summer monsoon intensity. By comparison of the composites of the periods of increasing and decreasing precipitation, we see that monsoon intensity induced by the seasonal reversal of low-level circulation is different, especially in the summer season. During the summers of periods of increasing precipitation, the southeasterly flow that sweeps over Korea is evident, in-
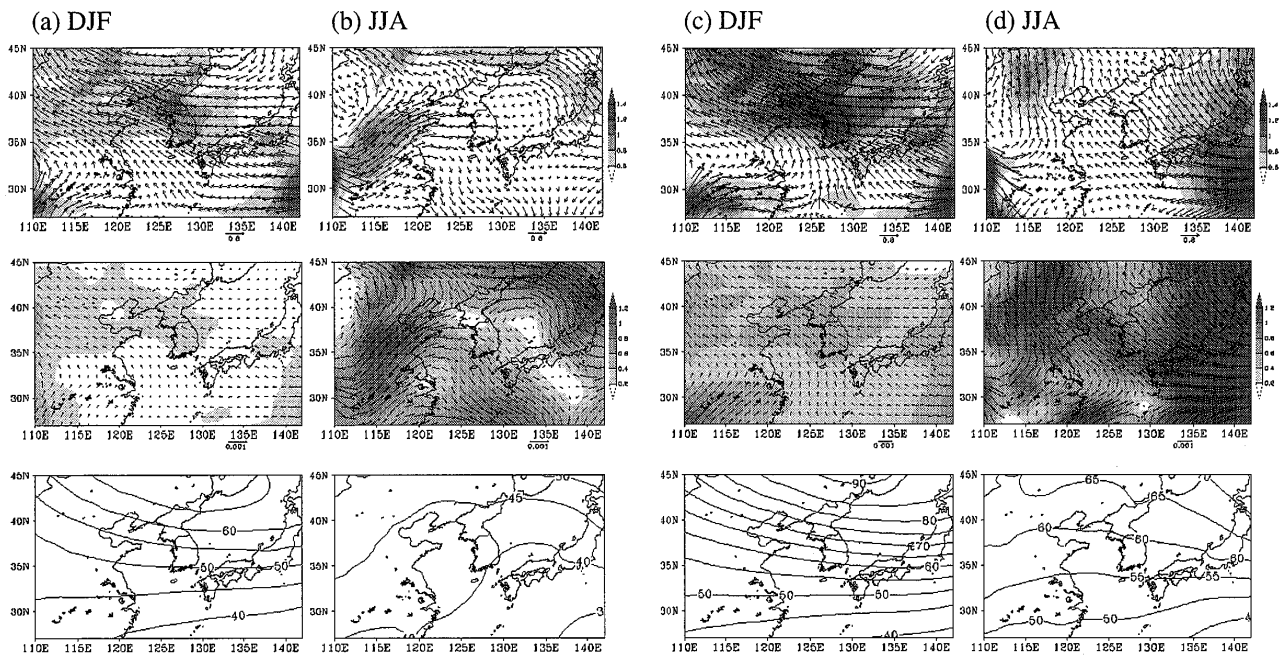

Fig. 3. Composite analysis of difference between precipitation decrease (2031–2040, 2061–2070) and increase (2051–2060, 2071~2080) periods and reference simulation (1971~2000) in the 850 hPa winds (upper panels), 850 hPa water vapor flux (middle panels), and 500 hPa geopotential height (lower panels) for winter (a and c) and summer (b and d) season over East Asia. Shading indicates the magnitude of wind (upper panels) and water vapor flux (middle panels).

dicating an overall intensification of monsoonal activity in summer. The increased southeasterlies are favorable for advection of lower level warm and moist air from the Pacific Ocean, resulting in more precipitation (Lu et al. 2007). In winter the prominent feature is related to the weakening of the East Asian monsoon circulation due to a reduction of the land-sea contrast, leading to a weakening of the prevailing northwesterly flow. Both composite features show a similar wave pattern of weakening of the northwesterly flow, but the magnitude is more pronounced during periods of increased precipitation.

By comparison between wind fields and water vapor flux in the 850 hPa height, the change in the wind field mainly contributes to the change in the water vapor flux, which is a key factor to the change in the precipitation. Based on the wind fields for summer season, the strongest flux vectors curve anticyclonically along the west margin of the western Pacific high in periods of increasing precipitation while the strongest flux vectors come predominately from China mainland in periods of decreasing precipitation. During the wet period, main transport branch from Pacific Ocean intensify summer monsoon bringing abundant moisture over Korea.

The increase in the 500 hPa height reflects the greenhouse warming under enhanced GHG concentrations, in which the atmosphere holds more water vapor. The positive signal in the 500 hPa height due to warming is similar in both composite members. However, the heights during periods of increased precipitation show larger magnitude and a stronger gradient which is likely to represent a stronger warming signal.

Recent studies show that East Asia is likely to experience a warmer and wetter climate over the 21st century with stronger amplitudes than in the global mean change using global projection results (Min et al. 2006; Kripalani et al. 2006). Particularly, it is reported that the internal variability and uncertainty are larger in the regional precipitation than in the global precipitation. This implies that the uncertainty is increasing as the temporal and spatial scales are reduced. In order to examine the seasonal and regional dependency of climate change, the area-averaged seasonal mean change over East Asia (mother domain simulation) and Korea (nested domain simulation) are shown for four seasons (DJF, MAM, JJA, and SON) and annual mean (ANN) (Fig. 4). Here, the error-bar represents interannual variability measured by the standard deviation of the seasonally averaged temperature and precipitation. For temperature change, we notice that increases in both regions during 2051–2080 are much larger than those during 2021–2050. Moreover, the seasonal dependency of the pattern of temperature change is also intensified, especially over Korea. In the winter season during 2051–2080, the temperatures increase up to 3.0 K and 3.3 K over East Asia and Korea, respectively. All temperature change signals consistently exceed the interannual variability, which implies robustness of the signal. A pronounced increase of the mean value in the late twenty-first century indicates that the warming signal becomes more pronounced as the GHG concentration is increased.

Moving to the seasonal precipitation variation, considerable difference between precipitation and temperature is found in terms of interannual variability. Unlike temperature, the variability of precipitation ranges widely across regions and seasons, consistently exceeding the mean change. Since a spatially discontinuous variable such as precipitation has a greater location dependency than does temperature (Mearns et al. 1984), it might be natural that seasonal estimates of precipitation changes are more unreliable than those of temperature. In spite of a very large uncertainty in the projection, the seasonal change in precipitation has an overall increase, especially in the cold season. During 2051–2080, winter precipitation over Korea increased by about 40%. Accordingly, the enhancement of winter precipitation over Korea is generally considered a very likely future consequence of climate change. The variability over Korea is much larger than that of East Asia. It means that the uncertainty increases as the scale of interest becomes finer and closer to that needed for impact assessment studies, since the variability also increases at finer scale (Giorgi 2005).

In order to address the issue of statistical significance of the change in seasonal and annual mean temperature and precipitation with respect to the reference simulation (1971–2000)
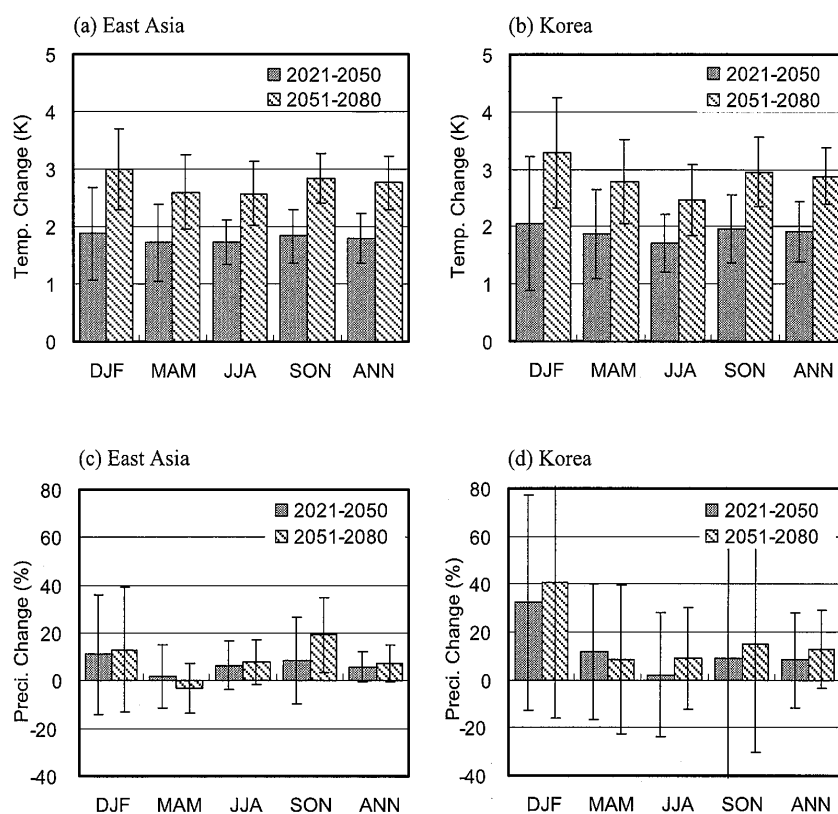
Fig. 4. Seasonal mean change of area-averaged temperature and precipitation over East Asia and Korea and their interannual variability for the two futures (2021–2050 and 2051–2080) relative to reference (1971–2000). The units of temperature and precipitation change are K and %, respectively.

as shown by Fig. 4, we perform a two-tailed t-test assuming unequal variances (Welch's t-test). For both East Asian (mother domain simulation) and Korean region (nested domain simulation), and for both future periods (2021–2050/2051–2080), the change in mean temperature was very significant, with p-values below 10^{-8} for all seasons as well as annual mean. The p-values represent the probability that the absolute value of the test statistic exceeds that

calculated for the future and reference scenario by random chance. For precipitation, we have less confidence. The p-values obtained from the t-test for precipitation are given in Table 1. For East Asian region, the change in precipitation is significant at the 5% level or lower ($p < 0.05$) for JJA, and annual mean for the 2021–2050 period, and for JJA, SON, and annual mean for the 2051–2080 period. For the Korean region, the change in precipitation was

Table 1. P-values of a two-tailed t-test assuming unequal variances between simulated seasonal and annual mean precipitation for both regions and for both future periods. Values in bold indicates significant at the 5% level.

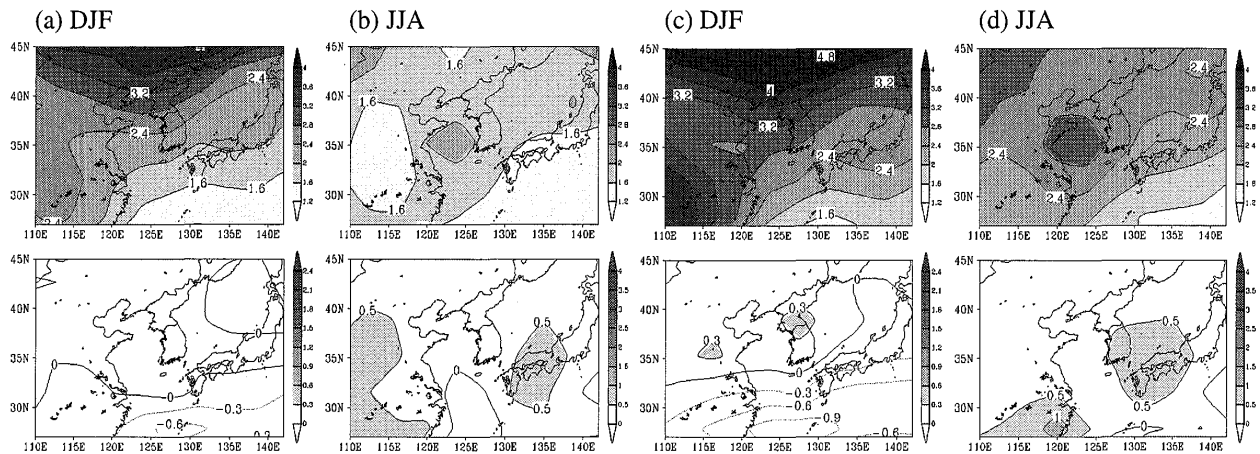|		DJF	MAM	JJA	SON	ANN
East Asia	2021–2050	0.1172	0.6281	**0.0154**	0.1052	**0.0015**
	2051–2080	0.0733	0.3195	**0.0026**	**0.0002**	**0.0004**
Korea	2021–2050	**0.0033**	0.0612	0.7521	0.4538	0.0806
	2051–2080	**0.0017**	0.2048	0.1453	0.1865	**0.0034**

Fig. 5. Difference between future scenarios (2021–2050 and 2051–2080) and reference simulation (1971–2000) temperature (upper panels) and precipitation (lower panels) in ECHO-G run for winter (a and c) and summer (b and d) season. Units are K and mm/day.

significant at the 5% level or lower for DJF for the 2021–2050 period, and for DJF and annual mean for the 2051–2080 period.

Figures 5 and 6 present the spatial distribution of differences between the future and reference scenarios in surface air temperature and precipitation over East Asia computed from the ECHO-G and RegCM3 mother domain simulation. Although the large-scale circulations in the regional climate simulation and driving fields are very similar, the regional details of the simulated surface changes can be quite difference due to the effects of local topographical and land use features (Im et al. 2007a). By comparison of the two future-period simulations, we find the change signal becomes more intensified in the late twenty-first century as global warming undergoes, even though both simulations are essentially the same in terms of the spatial distribution.

For temperature, substantial warming is evident, and larger at higher latitudes in winter with consistent pattern. In the cold season (DJF), significant warming is found over almost the entire region, indicating excess of 4 K over the northern areas of the Korean Peninsula
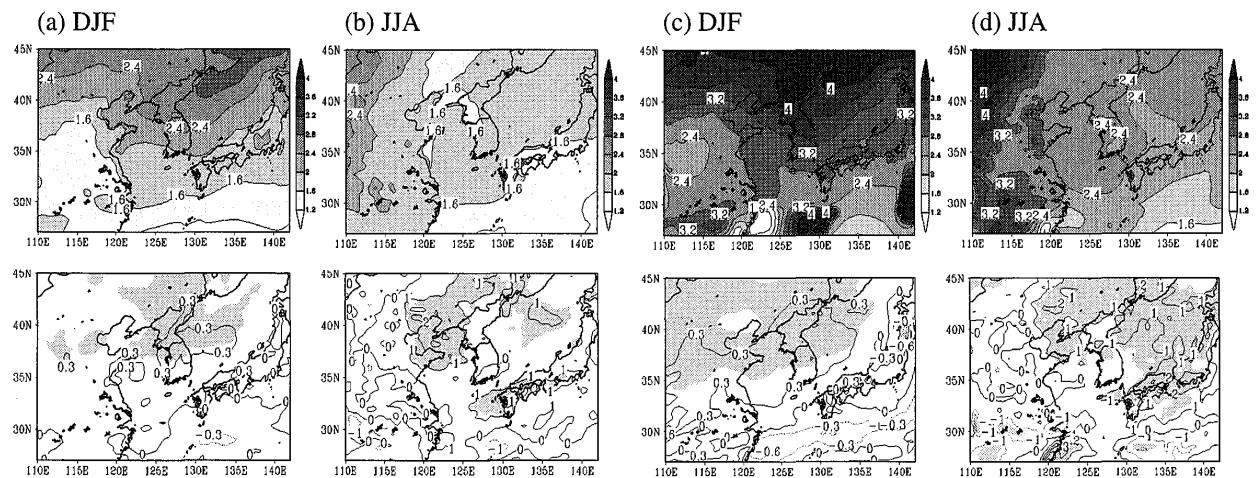

Fig. 6. Difference between future scenarios (2021–2050 and 2051–2080) and reference simulation (1971–2000) temperature (upper panels) and precipitation (lower panels) in RegCM3 mother domain run for winter (a and c) and summer (b and d) season. Shading in precipitation indicates statistically significant at the 90% and 70% confidence level for winter and summer season. Units are K and mm/day.

during 2051–2080. The regional model shows a surface warming pattern similar to that of ECHO-G, with a strong positive northward gradient. The magnitude of the surface warming is, however, smaller in the mother domain simulation than in ECHO-G by 0.5–1.2 K. In particular, over central mainland China, the mother domain simulation shows considerably less warming as compared to the ECHO-G simulation. This difference is probably associated with differences in the simulated changes in the surface variables such as snow cover and soil water content (Im et al. 2007b). Significant regional differences are also observed between the summer warming patterns of the ECHO-G and mother domain simulations, even though warming is evident throughout the entire integration area. ECHO-G shows a maximum over the Yellow Sea, while the mother domain simulation shows a maximum along the western boundary region. Furthermore, as can be expected, the gradients in the warming patterns are much sharper and more complex in the regional model simulation than in ECHO-G.

In contrast to the temperature, changes in precipitation are unclear and a relatively large spread in both periods exists. The regional deviation is also larger than for the temperature fields. Lack of spatial details for ECHO-G simulation is highlighted. It can be noted that, even for the 30-year average, the precipitation change pattern in the regional model exhibits a much greater fine scale structure than that in the global model simulation especially summer season, although this variability does not seem to be tied to specific topographic features of the region. For winter precipitation, even though both simulations project the precipitation increase over broad area, the area of increase is more expanded in the mother domain simulation. In particular, a distinct large increase is observed over the central region including the entire Korean Peninsula. It is very likely that the precipitation increase during winter season is due to enhance water-holding capacity of the warmer atmosphere based on the Clausius-Clapeyron relation. Greater differences between the ECHO-G and mother domain simulations are found for the change in the summer monsoon precipitation. In the ECHO-G simulation, one of the largest increases in precipitation occurs over central

and southern mainland China, while in the mother domain simulation, the largest increase in monsoon precipitation occurs over north-east China. Previous regional modeling experiments (e.g., Deque et al. 2005) have shown that the lateral boundary forcing exerts a relatively weak control on a nested model solution during summer, when local processes such as land-atmosphere interactions and especially moist convection play a major role in determining precipitation.

The detailed structures of future change of surface climate over Korea produced from the nested domain simulations are illustrated in Fig. 7. The general patterns are along the lines of those found in the mother domain simulations. An important aspect of the changes from the nested domain simulation is the fine scale structure of the change signal associated with coastlines and topography. The temperature warming signal is amplified over the cold region during the winter, showing a strong northward gradient. One possible explanation of the warming amplification in the cold season has been attributed, at least partially, to snow reduction (Im et al. 2007b), and the resulting snow-albedo feedback mechanism (Giorgi et al. 1997), which increases the absorption of heat at the surface where snow cover is significantly less. It can be clearly seen in our scenario that in areas where the snow decreases, there is an increase in solar absorption due to a decreased albedo. The spatial pattern correlation between the snow depth and the clear-sky surface absorbed solar flux change is −0.89 (See Figs. 9 and 10 in Im et al. 2007b). During the summer, temperature change intensity is less evident and spatial pattern is more uniform across the Korean Peninsula domain.

The amount of winter precipitation tends to increase during 2021–2050 relative to 1971–2000, and the intensity become more evident during 2051–2080. When looking at the spatial distribution, the maximum along the north-eastern coastal ranges is likely to be a detailed orographic effect in response to topographic uplifting of on-shore moist flow. The change of summer precipitation has a more complex distribution. The changes in seasonal precipitation are likely due to different mechanisms between the warm and cold season. In the cold season precipitation is produced by large-scale
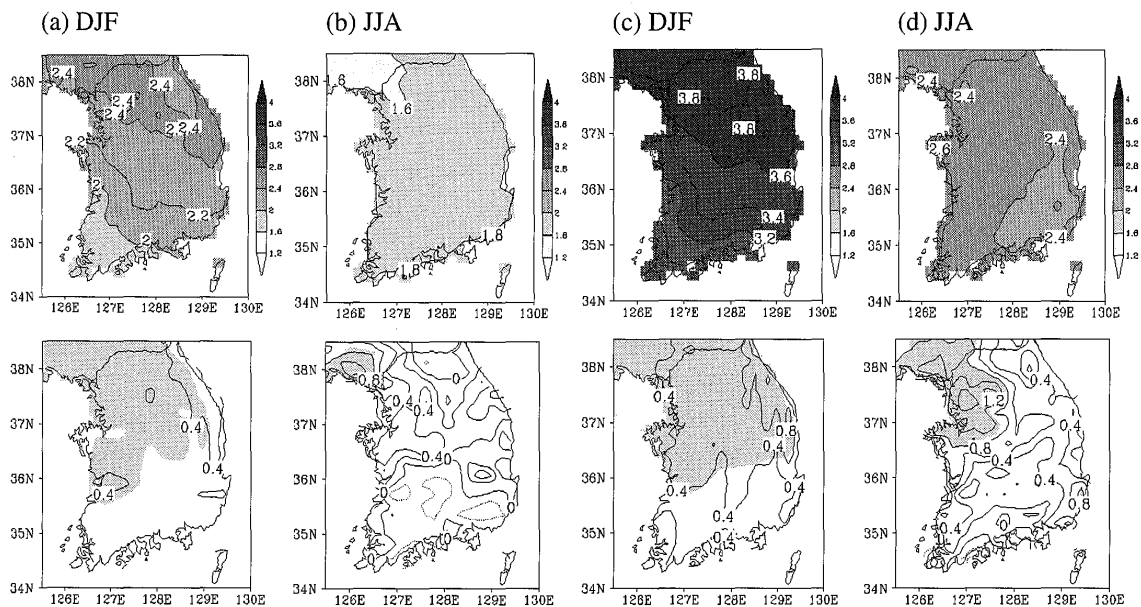
Fig. 7.   Same as Fig. 6, except for the nested domain simulation.

circulation under strong baroclinicity conditions, whereas in summer the rain is produced by more complicated phenomena such as typhoons, tropical storms, and monsoon convective systems (Im et al. 2006). The southern parts of Korea during 2021–2050 will be expected to have dry conditions, whereas precipitation during 2051–2080 is projected to increase over whole area, with a maximum in northwest region.

We carried out a two-tailed t-test to calculate the statistical significance of these changes projected by RegCM3. In Figs. 6 and 7 the shading in precipitation indicates the areas where the change is statistically significant at the 90% (winter) and 70% (summer) confidence level. The temperature changes are statistically significant at the 90% confidence level in all seasons and over the entire analysis area (not indicated by shading). For the precipitation in mother domain, although the significant regions are restricted to a small part of the simulated area, shading areas become extended in the late twenty-first century. In the nested domain, the change signal is more mixed. In winter, the area of statistically significant increase is widespread across northern part of South Korea while in summer, most of the projected precipitation changes show low statistical confidence, probably because of the large natural variability. This makes it very difficult to arrive

at any general interpretation. This uncertainty is commonly revealed in future projection experiments using state-of-the-art high resolutions in both regional and global climate models (Leung et al. 2004; Kusunoki et al. 2006), indicating a significant diversity among model results. This problem justifies the need for further ensemble experiments of various kinds (e.g., emission scenarios, global model driving fields, initial conditions, and so on) to reduce the uncertainty, which could provide more promising climate scenario information.

In summary, Figs. 2–7 indicate that there are predominant change signals present over East Asia including the Korean Peninsula in response to global warming. The amplitude as well as the uncertainty of change signal are intensified over Korea relative to that over East Asia, showing a strong seasonal and regional dependency. Enhanced GHG is very likely to lead to increased temperature and precipitation in the spatial and temporal mean senses, but its geographical distribution is not directly responded to the increase of the GHG, in particular with respect to precipitation (Kitoh et al. 2005). The projected temperature and precipitation from the regional modeling system demonstrate the greater spatial detail due to the effect of local topographical features over Korea. On the other hand, these features are not found in the ECHO-G simulations which

are used as initial and boundary conditions. It well illustrates the need for high resolution in regions characterized by complex topography. In addition, climate change scenarios based on linearly interpolated output from a GCM (typical horizontal grid spacing ~ 300 km) are unlikely to be adequate for use in regional impact studies (Johns et al. 1997).

In the next section, we turn our attention to the analysis of daily properties for further understanding of the characteristics related extreme events in more detail.

3.2 Changes in daily properties

Global warming would result in not only changes in mean climatology but also in the increase in frequency and intensity of extreme events on daily time scales (Kitoh et al. 2005). Therefore, the change of daily properties of the relevant climate variables is investigated. Here, we convert model grid data to 57 station data at the grid point closet to the observed station locations over the Korean territory (Im et al. 2007a).

We first examine the probability density function (PDF) of temperature fields, including a measure of the central tendency (e.g., the mean) and a measure of dispersion (e.g., the standard deviation or variance) (Leung et al. 2004). Figure 8 shows the PDF of the distribution of the daily mean, maximum, and minimum temperature. Among them, the distribution range is different while the fundamental shape is similar. The shape of annual PDF exhibits a bimodal structure reflecting seasonal characteristics for the cold season (lower and broader distribution) and the warm season (higher and narrower distribution). There is a common tendency of a shift to a higher mean values in the future climate than that during the reference period, suggesting increased milder conditions due to greenhouse warming. The change range during 2021–2050 with respect the reference simulation shows to be much higher than that of 2051–2080. Compared to the change of the mean value in the future, change of the dispersion appears to be negligible. Accordingly, there is an increase in the number of extreme hot days and a decrease in the number of extreme cold days. These features are clearly revealed in the hot and frost spell distributions (See Fig. 10).
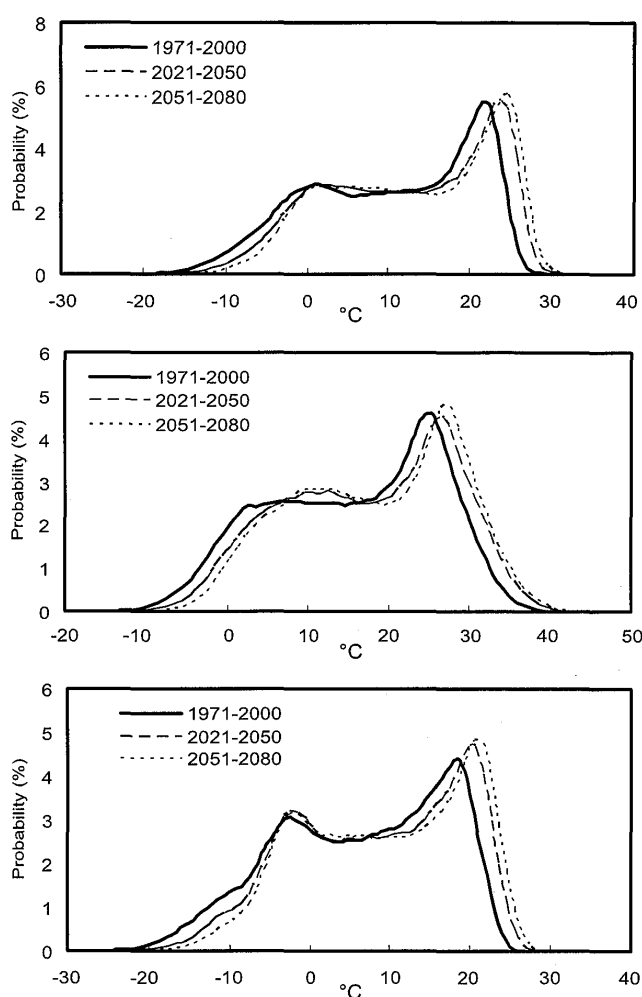

Fig. 8. Probability density function of the annual distribution of daily mean (upper), maximum (middle), and minimum (lower) temperature in Korea.

Figure 9 shows frequency distribution of daily precipitation in 5 mm/day intervals for 1970–2000 (reference scenario), 2021–2050 and 2051–2080 for 57 stations. It can be seen that there is an increase in precipitation events in nearly all bin intervals for the future scenarios, with the 2051–2080 scenario showing the largest increase in all intervals. To assess statistical significance, we first note that if all precipitation events for all stations are considered independent, then the number of events is sufficiently large that a Chi square test gives a p-value $< 10^{-10}$ for both future scenarios tested against the reference scenario. Therefore we must reject the null hypothesis that the future projections have the same distribution as the reference scenario. However, precipitation is
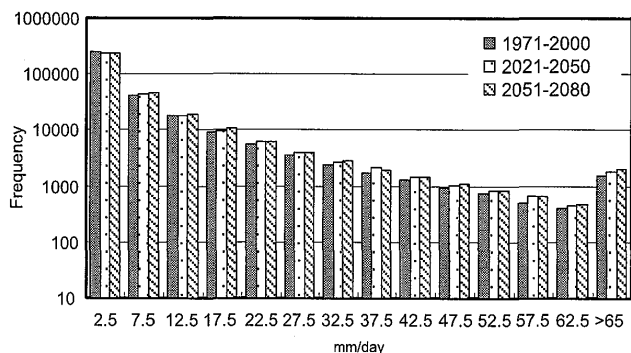
Fig. 9. Frequency distribution of daily precipitation in 5 mm/day intervals in Korea.

often associated with large scale systems, and hence there is likely some dependence amongst the stations due to their relatively close proximity. If we assume that the stations are completely dependent, a Chi square test gives a p-value of 0.7 for the 2021–2050 period, and $p < 10^{-10}$ for the 2051–2080 period. Thus, for the far future, 2051–2080, the daily precipitation distribution is significantly different statistically from the reference scenario even under the conservative assumption of complete dependence. For the near future, 2020–2050, we cannot reject the null hypothesis, and more detailed analysis of station interdependence is needed in order to assess statistical significance. However, given that the near future scenario results are intermediate between the reference and far future scenario results, it is reasonable to assume the increase in precipitation in the near future scenario is likely significant.

In this study, we also attempt the 'series' approach using daily data in terms of the sequences of wet/dry and frost/hot days. Because persistence of weather events may lead to extremes such as flood, drought and so on, successive events of various durations can reveal significant structure of the frequency and intensity of extremes (Halenka et al. 2006). The four categories of spells used in this study are calculated as a number of consecutive days as follows. A wet day is defined as a day with precipitation accumulation greater than or equal to 1.0 mm, and at least one dry (wet) day is referred to as a dry (wet) spell. A frost day is defined as a minimum temperature less

than 273.15 K (0°C), while a hot day occurs if the maximum temperature exceeds 303.15 K (30°C). All spells are divided into 9 duration intervals. Each duration interval is empirically chosen based on the expected properties of the weather variables, as interval size gradually increases (Im and Kwon 2007).

Figure 10 presents the potential future change (2021–2050 and 2051–2080) of frequency of the frost and hot spell for various durations with respect to the reference (1971–2000). The lines in Figure 10 indicate daily minimum/maximum temperature in the frost/hot spells averaged over the spells of each duration class. The projected frost and hot spells indicate a significant warming in the frequency as well as the intensity. An increase in the number of hot days has been projected over Korea, along with increasing mean maximum temperature except for the 13–26 day duration
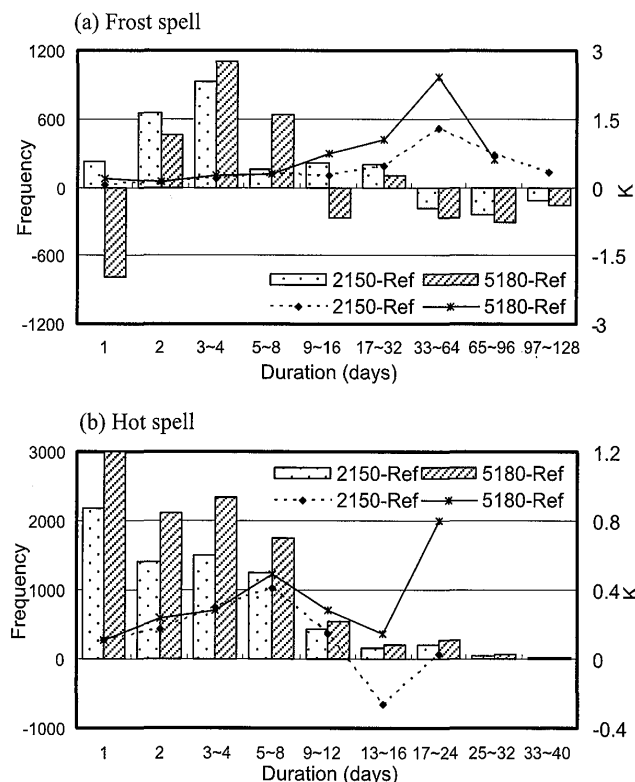

Fig. 10. Future change of frequency distribution of the frost and hot spells of various durations. Here, the lines for the frost/hot spell indicate the daily minimum/maximum temperature averaged over the spells of each duration class.

during 2021–2050. At the same time, episodes of severely successive cold days may become less frequent in the milder future climate. Relatively short period frost spells are likely to increase due to breaks of long spells by greenhouse warming. However, extreme frost spells exceeding 33 days tend to decrease and extreme frost spells exceeding 96 days would essentially vanish during 2051–2080. In addition, a substantial increase of minimum temperature is found throughout the whole duration, in particular exceeding 2 K during 2051–2080. The increasing trend of projected temperature due to anthropogenic forcing is associated with an increase (decrease) in the number of hot (frost) days as well as corresponding maximum (minimum) temperature.

Regarding the dry and wet spells related to daily precipitation (Fig. 11), the dry spell change does not reveal any significant trend, but shows the reduction in events less than 3 days. On the other hand, the enhancement in the relatively intensive events exceeding 4 days is evident in the wet spells. As indicated

by the averaged daily precipitation for each duration, an increase of precipitation intensity is projected in the future except for the 3–24 day duration (2021–2050) and 6 day duration (2051–2080). The results suggest the possibility that precipitation intensity in the future may increase in response to anthropogenic forcings, and appears in line with results found in other regional climate change projections for the 21st century (Boo et al. 2006; Gao et al. 2006).

4. Summary and discussions

In this study, we investigate possible future climate changes with a focus on the Korean Peninsula under forcing from the IPCC SRES B2 emission scenario. For simulating the fine-scale climate change scenario, a one-way double-nested regional climate model system using RegCM3 has been applied to the ECHO-G (ECHAM4/HOPE-G) global climate model of approximately 350 km horizontal resolution. In order to consider the interdecadal variability of the model, a total 110-year simulation period of 1971–2080 is performed. The comparison between 2021–2050 and 2051–2080 is key for assessing climate change at different time periods in response to anthropogenic forcings.

Projected changes in both temperature and precipitation fields provide strong evidence that East Asia including the Korean Peninsula undergoes a warmer and wetter climate regime in response to the intensification of the summer monsoon and weakening of the winter monsoon. The magnitude of the change signals both in mean and extremes of temperature and precipitation in response to anthropogenic forcings is more pronounced in 2051–2080 compared to the period of 2021–2050 as GHG concentration increased. The temperature exhibits a positively persistent trend throughout whole period increasing by 3.2 K for 2070s while precipitation is characterized by pronounced interdecadal variations, with gradual amplification of the fluctuation range. During wet periods, the summer monsoon is intensified due to stronger southeasterly flow, favorable for advection of lower level warm and moist air from the Pacific Ocean. The temperature changes are statistically significant with robustness regardless of region and season while the precipitation changes show the low statistical con-
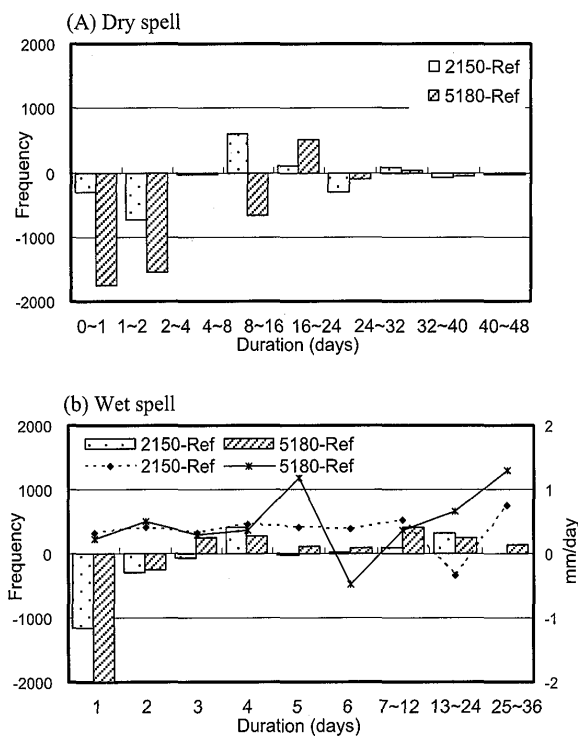

Fig. 11. Same as Fig. 10, except for dry and wet spells. Here, the lines for wet spell indicate the daily precipitation averaged over the spells of each duration class.

fidence due to large variability. A significant increase (decrease) of hot (frost) spells is found along with increasing of maximum and minimum temperature. Wet spells of long periods tend to be more frequent as well, accompanied with an increase of precipitation amounts.

Although it cannot be expected that a single realization in this study can establish the robustness of the regional change signal due to large uncertainties, these results could provide useful information for impact assessment as well as a plausible interpretation for the future climate, considering the reasonable verification of the reference scenario (Im et al. 2007a; Im and Kwon 2007).

Large scale forcing arising from global warming may lead to local changes of the surface climate over complex terrain regions such as the Korean Peninsula. A substantial change in the fine scale pattern of the climate is found across Korea, which justifies the need for high resolution modeling over the region. The nested model added more realistic detail to the simulated surface climatology due to its better representation of topography and coastlines. This work has demonstrated the feasibility of the nested modeling methodology for regional climate studies. Two of the main limitations of this work have been the use of a single projection, which prevents an accurate treatment of emission scenarios with large uncertainty, and the shortcomings in the quality of the driving GCM fields. In the near future, we will attempt a time-slice experiment of a high resolution GCM for providing higher-quality driving fields based on the various emission scenarios, which should result in more accurate nested model simulations for application to climate change studies.

Acknowledgements

References

Boo, K.-O., W.-T. Kwon, and H.-J. Baek, 2006: Change of extreme events of temperature and precipitation over Korea using regional projection of future climate change. *Geophys. Res. Lett.*, **33**, L01701, doi:10.1029/2005GL023378.

Boo, K.-O., W.-T. Kwon, J.-H. Oh, and H.-J. Baek, 2004: Response of global warming on regional climate change over Korea: An experiment with the MM5 model. *Geophys. Res. Lett.*, **31**, L21206, doi:10.1029/2004GL021171.

Christensen, O.B., J.H. Christensen, B. Machenauer, and M. Botzet, 1998: Very high-resolution regional climate simulations over Scandinavia Present climate. *J. Climate*, **11**, 3204–3229.

Deque, M., G. Jones, M. Wild, F. Giorgi, J.H. Christensen, D.C. Hassell, P.L. Vidale, B. Rockel, D. Jacob, E. Kjellstrom, M. de. Castro, F. Kucharski, and B. van den Hurk, 2005: Global high resolution versus Limited Area Model climate change projections over Europe: quantifying confidence level from FRUDENCE results. *Clim. Dyn.*, **25**, 653–670.

Fu, C.B., 2003: Potential impacts of human-induced land cover change on East Asia monsoon. *Global and Planetary Change*, **37**, 219–229.

Gallardo, C., A. Arribas, J.A. Predo, M.A. Gaertner, and M.D. Castro, 2001: Multi-year simulations using a regional-climate model over the Iberian Peninsula: Current climate and doubled CO_2 scenario. *Quart J. Roy. Meteor. Soc.*, **127**, 1659–1681.

Gao, X., J.S. Pal, and F. Giorgi, 2006: Projected changes in mean and extreme precipitation over the Mediterranean region from a high resolution double nested RCM simulation. *Geophys. Res. Lett.*, **33**, L03706, doi:10.1029/2005GL024954.

Gao, X., Z. Zhao, Y. Ding, R. Huang, and F. Giorgi, 2001: Climate change due to greenhouse effects in China as simulated by a regional climate model. *Adv. Atmos. Sci.*, **18**, 1224–1230.

Giorgi, F., 2005: Interdecadal variability of regional climate change: implications for the development of regional climate change scenarios. *Meteor. Atmos. Phys.*, **89**, 1–15.

Giorgi, F. and L.O. Mearns, 1999: Introduction to special section: Regional climate modeling revisited. *J. Geophys. Res.*, **104**, 6335–6352.

Giorgi, F., J.W. Hurrell, and M.R. Marinucci, 1997: Elevation dependency of the surface climate change signal: A model study. *J. Climate*, **10**, 288–296.

Giorgi, F., M.R. Marinucci, and G.T. Bates, 1993a: Development of a second generation regional climate model (RegCM2). Part I. Boundary-layer and radiative transfer processes. *Mon. Wea. Rev.*, **121**, 2794–2813.

Giorgi, F., M.R. Marinucci, G.T. Bates, and De Canio

G., 1993b: Development of a second generation regional climate model (RegCM2). Part II. Convective processes and assimilation of lateral boundary conditions. *Mon. Wea. Rev.*, **121**, 2814–2832.

Giorgi, F., X. Bi, and J. Pal, 2004a: Mean, interannual variability and trends in a regional climate change experiment over Europe. I: Present-day climate (1961–1990). *Clim. Dyn.*, **22**, 733–756.

Giorgi, F., X. Bi, and J. Pal, 2004b: Mean, interannual variability and trends in a regional climate change experiment over Europe. II: Climate change scenarios (2071–2100). *Clim. Dyn.*, **23**, 839–858.

Giorgi, F., X.Q. Bi, and Y. Qian, 2002: Direct radiative forcing and regional climate effects of anthropogenic aerosols over East Asia: A regional coupled climate-chemistry/aerosol model study. *J. Geophys. Res.*, **107**, 4439, doi:10.1029/2001JD001066.

Giorgi, F., X.Q. Bi, and Y. Qian, 2003: Indirect vs. direct effects of anthropogenic sulfate on the climate of East Asia as simulated with a regional coupled climate-chemistry/aerosol model. *Clim. Change*, **58**, 345–376.

Halenka, T., J. Kalvova, Z. Chladova, A. Demeteova, K. Zemankova, and M. Belda, 2006: On the capability of RegCM to capture extremes in long term regional climate simulation cumparison with the observations for Czech Republic. *Theor. Appl. Climatol.*, **86**, 121–142.

Im, E.-S. and W.-T. Kwon, 2007: Characteristics of extreme climate sequences over Korea using a regional climate change scenario. *SOLA*, **3**, 17–20.

Im, E.-S., E.-H. Park, W.-T. Kwon, and F. Giorgi, 2006: Present climate simulation over Korea with a regional climate model using a one-way double-nested system. *Theor. Appl. Climatol.*, **86**, 187–200.

Im, E.-S., W.-T. Kwon, J.-B. Ahn, and F. Giorgi, 2007a: Multi-decadal scenario simulation over Korea using a one-way double-nested regional climate model system. Part 1: Recent climate simulation (1971–2000). *Clim. Dyn.*, 28, 759–780.

Im, E.-S., J.-B. Ahn, W.-T. Kwon, and F. Giorgi, 2007b: Multi-decadal scenario simulation over Korea using a one-way double-nested regional climate model system. Part 2: Future climate projection (2021–2050). *Clim. Dyn.*, DOI 10.1007/s00382-007-0282-5.

IPCC, 2000: *Special Report on Emissions Scenarios. A Special Report of Working Group III of the Intergovernmental Panel on Climate Change* (Nakicenovic, N., J. Alcamo, G. Davis, B. devries, J. Fenhann, S. Gaffin, K. Gregory, A. Grubler, T. Yong Jung, T. Kram, E.L. La Rovere, L. Michaelis, S. Mori, T. Morita, W. Peper, H. Pitcher, L. Price, K. Riahi, A. Roehrl, H.-H. Rogner, A. Sankovski, M. Schlesinger, P. Shukla, S. Smith, R. Swart, S. van Rooijen, N. Victor, and Z. Dadi (eds.)). Cambridge University Press, Cambridge, UK, 599 pp.

IPCC, 2001: *Climate Change 2001: The Scientific Bias. Contribution of Working Group I to the Third Assessment Report of the Intergovernmental Panel on Climate Change* (Houghton, J.T., Y. Ding, D.J. Griggs, M. Noguer, P.J. van der Linden, X. Dai, K. Maskell, and C.A. Johnson (eds.)). Cambridge Univ. Press, UK and New York, NY, USA, 881 pp.

Jones, R.G., J.M. Murphy, M. Noguer, and A.B. Keen, 1997: Simulation of climate change over Europe using a nested regional-climate model II: Comparison of driving and regional model responses to a doubling of carbon dioxide. *Quart. J. Roy. Meteor. Soc.*, **123**, 265–292.

Kitoh, A., M. Hosaka, Y. Adachi, and K. Kamiguchi, 2005: Future projections of precipitation characteristics in East Asia simulated by the MRI CGCM2. *Adv. Atoms. Sci.*, **22**, 467–478.

Kripalani, R.H., J.H. Oh, and H.S. Chaudhari, 2006: Response of the East Asian summer monsoon to doubled atmospheric CO_2: Coupled climate model simulations and projections under IPCC AR4. *Theor. Appl. Climatol.*, **87**, 1–28, doi:10.1007/s00704-006-0238-4.

Kusunoki, S., J. Yoshimura, H. Yoshimura, A. Noda, K. Oouchi, and R. Mizuta, 2006: Change of Baiu rain band in global warming projection by an atmospheric general circulation model with a 20-km grid size. *J. Meteor. Soc. Japan*, **84**, 581–611.

Kwon, W.-T., 2005: Current status and perspectives of climate change sciences. *J. Korean Meteor. Soc.*, **41**, 325–336 (In Korean with English abstract).

Leung, L.R., Y. Qian, X. Bian, W.M. Washington, J. Han, and J.O. Roads, 2004: Mid-century ensemble regional climate change scenarios for the Western United States. *Clim. Change*, **62**, 75–113.

Lu, R., Y. Li, and B. Dong, 2007: East Asian precipitation increase under the global warming. *J. Korean Meteor. Soc.*, **43**, 267–272.

May, W. and E. Roeckner, 2001: A time-slice experiment with the ECHAM4 AGCM at high resolution: the impact of horizontal resolution on annual mean climate change. *Clim. Dyn.*, **17**, 407–420.

Mearns, L.O., I. Bogardi, F. Giorgi, I. Matyasovszky, and M. Palecki, 1999: Comparison of climate change scenarios generated from regional climate model experiments and statistical downscaling. *J. Geophys. Res.*, **104**, 6603–6621.

Mearns, L.O., R.W. Katz, and S.H. Schneider, 1984: Extreme high-temperature events: Changes in their probabilities with changes in mean temperature. *J. Climate. Appl. Meteor.*, **23**, 1601–1613.

Meehl, G.A., F. Zwiers, J. Evans, T. Knutson, L. Mearns, and P. Whetton, 2000: Trends in extreme weather and climate events: Issues related to modeling extremes in projections of futureclimate change. *Bull. Amer. Meteor. Soc.*, **81**, 427–436.

Min, S.-K., E.-H. Park, and W.-T. Kwon, 2004: Future Projection of East Asia Climate Change from Multi-AOGCM Ensemble of IPCC SRES Scenario Simulations. *J. Meteor. Soc. Japan*, **82**, 1187–1211.

Min, S.-K., S. Legutke, A. Hense, U. Cubasch, W.-T. Kwon, J.-H. Oh., and U. Schlese, 2006: East Asian Climate Change in the 21st Century as Simulated by the Coupled Climate Model ECHO-G under IPCC SRES Scenarios. *J. Meteor. Soc. Japan*, **84**, 1–26.

Min, S.-K., S. Legutke, A. Hense, and W.-T. Kwon, 2005: Internal variability in a 1000-year control simulation with the coupled climate model ECHO-G. Part I: Near surface temperature, precipitation, and mean sea level pressure. *Tellus*, **57A**, 605–621.

Oh, J.-H., T. Kim, M.-K. Kim, S.-H. Lee, S.-K. Min, and W.-T. Kwon, 2004: Regional climate simulation for Korea using dynamic downscaling and statistical adjustment. *J. Meteor. Soc. Japan*, **82**, 1629–1643.

Pal, J.S., E.E. Small, and E.A.B. Eltahir, 2000: Simulation of regional-scale water and energy budgets: Representation of subgrid cloud and precipitation processes within RegCM. *J. Geophys. Res.*, **105**, 29,576–29,594.

Qian, Y., L.R. Leung, S.J. Ghan, and F. Giorgi, 2003: Regional climate effects of aerosols over China: modeling and observation. *Tellus*, **55B**, 914–934.

Räisänen, J., U. Hansson, A. Ullerstig, R. Doscher, L.P. Graham, C. Jones, H.E.M. Meier, P. Samuelsson, and U. Willen, 2004: European climate in the late twenty-first century: regional simulations with two driving global models and two forcing scenarios. *Clim. Dyn.*, **22**, 13–31.